35th Annual International Conference of the IEEE EMBS
Osaka, Japan, 3 - 7 July, 2013

Image Plane Positioning by Pneumatic Actuators for Ultrasound Guidance*

Toshio Yoshida, Shinya Onogi, Yuki Sugano, Shun Saito, Takashi Mochizuki, and Kohji Masuda, *Member, IEEE*

Abstract— **Image guided procedures such as percutaneous needle insertion or high intensity focused ultrasound, have become quite widespread. In images acquisition, ultrasound (US) is convenient to use in a conventional operating room, and inexpensive compared to CT and MRI. However, US requires to handle an US probe and do not have the base coordinate system. Therefore, intraoperative image position is unclear and cannot position to interested area. To address the issues, we have developed a robotic system based on US calibration and a probe scanning robot. In this study, to validate the implement system, positioning accuracy of an image plane was evaluated. Moreover, we developed an automated US guidance system with a conventional US probe. The system enables image plane positioning to visualize a therapeutic tool automatically. From the results, positioning accuracy of the image plane was 1.6 mm and 1.5 deg, maximally. In the phantom test, the error between the positions of the image plane and the mock needle was 2.5 mm and 0.9 deg. We have confirmed that the proposed system is greatly applicable for an intraoperative US guidance.**

I. Introduction

In the recent years, image guided procedures, e.g. percutaneous needle insertion and high intensity focused ultrasound, have been widely used in various surgical procedures to minimize patients' invasion. To monitor those procedures, CT and MRI are useful because of true 3D volumes but they are inconvenient in interventional or intraoperative procedures because of their costs, imaging delay, and large size to place in conventional operating rooms. On the other hand, ultrasound (US) cannot acquire images automatically because US probe has to be held and handled on surface of a patient's skin by an operator, despite it has advantages in less invasiveness, less expensiveness, lower imaging delay, and smaller in size than CT and MRI. That means that obtained images are in the 'floating' probe coordinate systems, and their relative position between the images is not clear. Therefore, automatic scanning of US probe with 3D positional information with high accuracy is expected where CT and MRI cannot be applied.

One of the methods to address the issues is automatic probe scanning system with a robot, which has been reported [1-5]. These studies enable to control the position and orientation of a US probe accurately. However, these robots have risk factors to apply in clinical settings because of heavy-weight and low back-drivability. Meanwhile, a robotic system which is mounting on a patient directly has been reported [6]. However, the robot is still heavy, 2.2 kg, for mounting use and does not have 6 degrees of freedom. Moreover, another issue of their robots is that they control a US probe tip position rather than an image plane position.

To address the issues, we have developed a robotic system that is lightweight and high back-drivability [7]. The robot can directly control the image position by using the fixed transformation between a US probe and an image plane based on US calibration technique [8-11]. In this study, we integrated a US guidance system with the robot to visualize a therapeutic tool in an echogram automatically. The system accuracy and feasibility were evaluated in phantom tests.

II. System Configuration

A. *Design and implementation*

The probe scanning robot (Fig. 1(a)) consists of a frame mechanism and a probe holding mechanism. The frame mechanism was designed as wire-driven parallel mechanism with six pneumatic actuators. The probe holding mechanism has a DC motor. The robot can control a US probe by 6 degrees of freedom (DOF): 5-DOF by the frame mechanism and 1 rotation by the probe holding mechanism. Both the mechanisms have optical markers. As for the wire actuator, McKibben pneumatic actuators (Fig. 1(b)) were selected because of its lightweight with adequate power, low impedance, and safety. The actuator is 4.5 g weight and can generate 130 N forces in 0.2 MPa pressure in maximum. The actuator is connected with an air-compressor via an electro-magnetic valve controlled by pressure feedback.

Next, the kinematics of the robot is explained. The pneumatic actuators are attached to the frame mechanism and

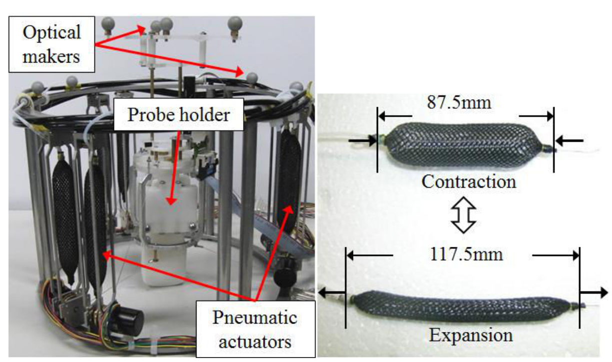

(a) Outlook (b) Actuator
Figure 1. Probe scanning robot.

*This research is supported by the Japan Society for the Promotion of Science (JSPS) through the Funding Program for Next Generation World-Leading Researchers (NEXT Program).

Toshio Yoshida, Shinya Onogi, Yuki Sugano, Shun Saito, Takashi Mochizuki and Kohji Masuda are with Graduate School of Bio-Applications and Systems Engineering, Tokyo University of Agriculture and Technology, Koganei, Tokyo, 184-8588 Japan (e-mail: 50012401319@st.tuat.ac.jp, {sonogi1, moch1302, masuda_k}@cc.tuat.ac.jp).

connected with the probe holding mechanism by wires via pulleys, respectively (Fig. 2). Here T is the transformation matrix. F represents the coordinates system of the frame mechanism and P represents the coordinates system of the probe. Both F and P are tracked by a tracking device. When a target probe position ${}^{F}T_{P}$ is given, the n-th target connecting point with the probe holding mechanism q_n is obtained as:

$$q_n = {}^{F}T_{P} Q_n, \tag{1}$$

where Q_n is the n-th initial connecting point with the probe holding mechanism (constant value) and n corresponds to a pneumatic actuator number, respectively (n=1~6). By the obtained points and the pulley positions, R_n, the wire lengths L_n to realize the target probe position are expressed as:

$$L_n = \left|\overrightarrow{R_n q_n}\right|. \tag{2}$$

Furthermore, the motor in the probe holding mechanism rotates the US probe around its axis.

B. Image plane position control

To manipulate an image plane position, the transformation matrix between a US probe and an image plane is required. Obtaining the transformation is generally referred as US probe calibration or US calibration. The position relationship between the coordinates is shown in Fig. 3. Here ΣFrame is the coordinates system of the frame mechanism, ΣProbe is the coordinates system of the probe, and ΣImage is the coordinates system of the image plane. When a target image plane position ${}^{F}T_{Im}$ is given, the target probe position ${}^{F}T_{P}$ is obtained as:

$${}^{F}T_{P} = {}^{F}T_{Im}\, {}^{Im}T_{P}, \tag{3}$$

where Im represents the coordinates system of the image plane and ${}^{Im}T_{P}$ is the US calibration matrix.

C. Integration of the robot with a US guidance

To capture movements of a therapeutic tool, the motion of the image plane is given by the following steps (Fig. 4).

(a) Translate the image plane to contain the therapeutic tool tip in the plane and y-axis of the plane. Here the transformation between the therapeutic tool and the image plane is required. The transformation is given by:

$${}^{Im}T_{Tool} = {}^{Im}T_{F}\, {}^{F}T_{Tool}, \tag{4}$$

where $Tool$ represents the coordinates system of the therapeutic tool, which was defined as follows: the origin is the tip position and the z-axis is the tool axis. Let a translation vector (p_x, p_y, p_z) be the translation component of ${}^{Im}T_{Tool}$. Thus, ${}^{F}T_{Im}$ is multiplied by TransZ(p_z)TransX(p_x). TransZ(z) is an abbreviation of a translation matrix in z-axis and TransX(x) is an abbreviation of a translation matrix in x-axis.

(b) Rotate the image plane around the axis, which direction is y-axis of the plane and passed through the therapeutic tool tip, to contain the therapeutic tool axis in the plane. Thus, ${}^{F}T_{Im}$ is multiplied by RotY(θ). RotY(θ) is an abbreviation of a rotation matrix around y-axis.

$$\theta = \sin^{-1}\left(\overrightarrow{n_{Im}} \times \overrightarrow{z'_{Tool}}\right), \tag{5}$$

where $\overrightarrow{n_{Im}}$ is the normal vector of the image plane (0, 0, 1), and $\overrightarrow{z'_{Tool}}$ is projection of the therapeutic tool axis to $X_{Im}Z_{Im}$-plane.

(c) Back the image plane only in x-axis. Thus, ${}^{F}T_{Im}$ is multiplied by TransX(-p_x).

(d) Finally, the target position of the image plane ${}^{F}T_{Im'}$ is obtained as:

$${}^{F}T_{Im'} = {}^{F}T_{Im}\,\mathrm{TransZ}(p_z)\,\mathrm{TransX}(p_x)\,\mathrm{RotY}(\theta)\,\mathrm{TransX}(-p_x). \tag{6}$$

According to the above formulas, the robot can automatically manipulate the position of the image plane to contain the therapeutic tool in the plane using X_{Im} and Z_{Im} translation, and Y_{Im} rotation of the image plane.

Navigation software including the above algorithm was developed using C++ (Visual Studio 2010, Microsoft) and the visualization toolkit (VTK 5.10.0, Kitware Inc.). Also, the software can communicate with the tracking device and the robot, and capture an echogram via a composite cable.

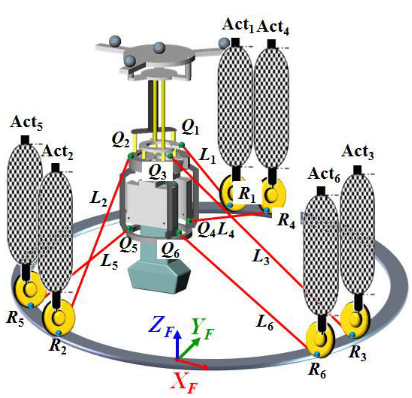

Figure 2. Configuration of pneumatic actuators.

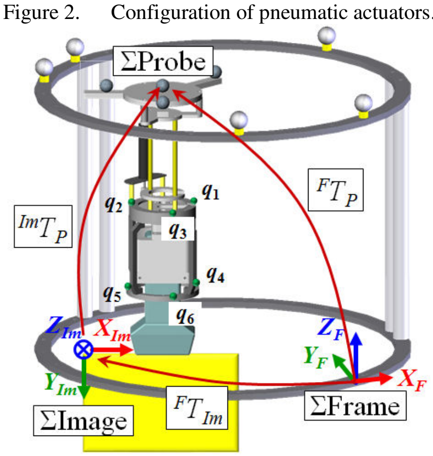

Figure 3. The position relationship between the coordinates.

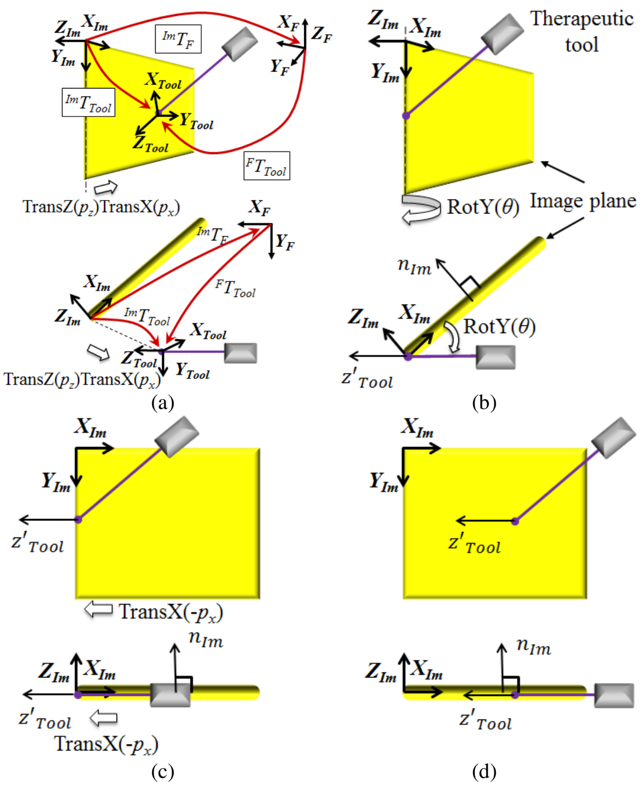

Figure 4. Motion of the image plane for the US guidance.

III. POSITION ACCURACY MEASUREMENT

To validate the image plane position control, positioning accuracy was measured by pivot motion of the image plane at X_F, Y_F, and Z_F axis (Fig. 5(a)). A phantom consisted of water and rubber (Fig. 5(b)). The phantom contained a metal ball with 5.5 mm radius as a mimic tumor. The probe scanning robot was fixed on the phantom, and the probe holding mechanism was placed vertically at the center of the robot. A pivot center was defined as the point under 70 mm distance from the frame bottom. The image plane was pivot around X_F axis and Y_F axis from -5.0 deg from 5.0 deg in the steps of 1.0 deg. The image plane was also pivot around Z_F from 0.0 deg to 90.0 deg in the steps of 1.0 deg. The position of the image plane was measured by the tracking device.

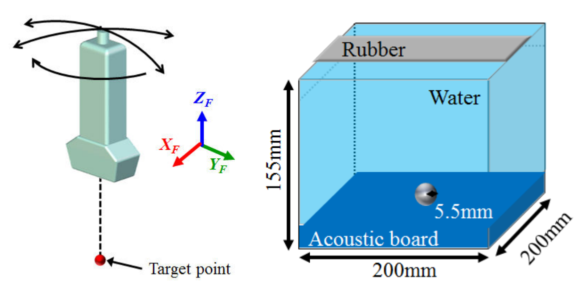

(a) Motion of the probe (b) Phantom

Figure 5. Experimental environment.

Fig. 6 shows average errors and standard deviations of pivot motion of the image plane in Frame coordinate system. From this result, the standard deviations were higher than the average errors, respectively. Table 1 shows root mean square errors (RMSE) of pivot motion of the image plane in Frame coordinate system.

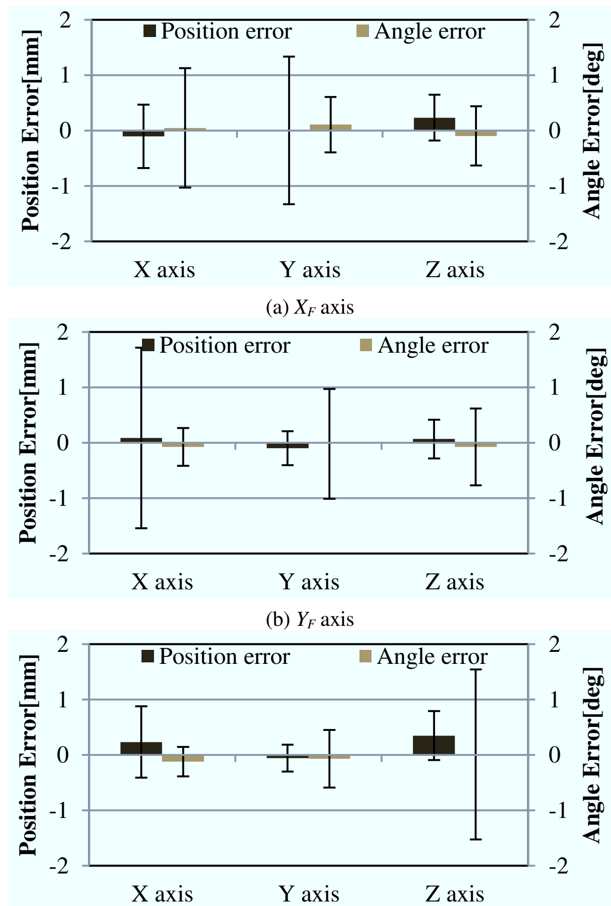

(a) X_F axis

(b) Y_F axis

(c) Z_F axis

Figure 6. Error of image plane position control.

TABLE I. RMSE OF PIVOT MOTION OF THE IMAGE PLANE IN FRAME COORDINATE SYSTEM

	position error[mm]			angle error[deg]		
	X	Y	Z	X	Y	Z
X_F axis	0.6	1.3	0.5	1.1	0.5	0.5
Y_F axis	1.6	0.3	0.4	0.3	1.0	0.7
Z_F axis	0.7	0.2	0.6	0.3	0.5	1.5

IV. US GUIDANCE EXPERIMENT

In this experiment, the probe scanning robot, a mock needle with optical markers, the tracking device, and the phantom were used. First, the tracked needle was calibrated by pivot motion. Next, the robot held a US probe and obtained the fixed transformation between a US probe and an image plane by US calibration [11]. RMSE of the US calibration was 2.3 mm. The calibration time was about 1 hour. Next, the robot was mounted on the phantom. After the initial setups, the needle was inserted to the phantom and manually moved as pivot motion in the phantom with the US guidance system. As for the evaluation, two types of errors were defined: one is the length of perpendicular to the image plane from the tip of the needle as a position error, and the other is the angle between the needle and the plane as an angle error.

Fig. 7 shows the US guidance views and the echograms during the experiment. In the US guidance views, the echogram planes and the needle model (green line) were shown in the 3-D space. The needle was also observed in the echogram as a high brightness line. From this result, we confirmed that the proposed system enables to guide a therapeutic tool in quasi-real-time. Table 2 shows RMSE of the defined errors.

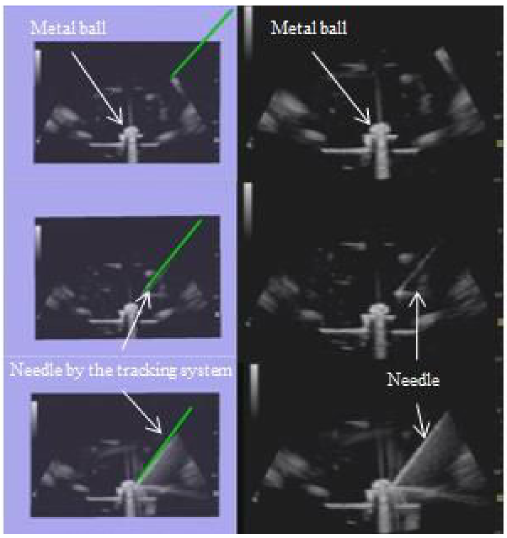

Figure 7. US guidance views and echograms during the experiment.

TABLE II. RMSE OF US GUIDANCE EXPERIMENT

	The length [mm]	The angle [deg]
RMSE	2.5	0.9

V. DISCUSSION AND CONCLUSION

In this study, we evaluated positioning accuracy of the image plane by the probe scanning robot. We also integrated the robotic system with a US guidance to monitor a therapeutic tool in an echogram without manual probe scanning. Moreover, the proposed system was validated by the US guidance experiment.

In accuracy evaluation, the positioning errors were less than 2.0 mm and 2.0 deg by the robot. The errors include following errors: kinematics and tracking. We consider that kinematics error include two error factors. First, we calculated kinematics of the robot by the wire connected position based on the mechanical design. And so, the robot positioning would have errors by the difference between the wire connected positions of the actual and the design. Second, the each characteristic of the pneumatic actuators was slightly different. Meanwhile, the tracking error (RMSE 0.3 mm) should be smaller than the kinematical error. In accuracy evaluation, a pivot center was defined as the point under 70 mm distance from the frame bottom. Generally, the thickness of the image plane (US beam width) at 70 mm distance is 4 mm, approximately. Thus, we consider that positioning accuracy is adequate for target imaging.

In the US guidance experiment, the proposed system was validated by two defined errors. First error was the length of perpendicular to the image plane from the tip of tracker and second error was the angle made the tracker to the image plane. The length was 2.5 mm and the angle was 0.9 deg. In the US guidance experiment, the mock needle was moved as pivot motion by manual. A pivot center was the point under about 120 mm distance from the frame bottom. The thickness of the image plane at 120 mm distance is about 7 mm. The proposed system enables to capture the needle automatically. However, a target such as a tumor etc. was not tracked at present. When the target was shift in body by deformation of soft tissues or breathes, the target may be lost from the echogram plane. One of method to address the issues is 3D-volume acquisition around the tracker by a 3D US probe.

We have considered several approaches for clinical use in the future work. The robot should be set near surface of a patient. Therefore, we have considered that two methods: one is that mount on a patient using belts, and the other is that cantilever-type jigs fixed to a bedside. In case of by belts, loads and fixedness would be issues. In case of by a jig, the robot has to follow motions of a patient.

In conclusions, we proposed a US guidance system with the robot to visualize a therapeutic tool in an echogram automatically. The proposed system enables to visualize the mock needle in an echogram automatically in the US guidance experiment. From the results, the proposed system has a great potential for an intraoperative US guidance system for less invasive therapy.

REFERENCES

[1] M. A. Janvier, L. G. Durand, Cardinal Roy, et al, “Performance evaluation of a medical robotic 3D-ultrasound imaging system,” Med. Image Anal. Vol. 12, pp. 275-290, 2008.

[2] R. Nakadate, H. Hirano, et al, “Development of Assisted-Robotic System Designed to Measure the Wave Intensity with an Ultrasonic Diagnostic Device,” in Proc. IEEE/RSJ Int. Conf. Intelligent Robots and Systems, pp. 510-515, 2009.

[3] P. Abolmaesumi, S. E. Salcudean, W. H. Zhu, S. P. DiMaio, M. R. Sirouspour, “A User Interface for Robot-Assisted Diagnostic Ultrasound,” in Proc. IEEE Int. Conf. on Robot. Autom.2001, 1549-1554.

[4] Y. Yu, T. Podder, Y. Zhang, W. Ng, V. Misic, J. Sherman, L. Fu, D. Fuller, E. Messing, D. Rubens, J. Strang, R. Brasacchio, “Robot-Assisted Prostate Brachytherapy,” MICCAI, LNCS 4190, pp. 41-49, 2006.

[5] N. Hungr, J. Troccaz, N. Zemiti, N. Tripodi, “Design of an Ultrasound-Guided Robotic Brachytherapy Needle-Insertion System,” in Proc. Annual Int. Conf. IEEE Eng. Med. Biol. Soc., pp. 250-253, 2009.

[6] K. Ito, S. Sugano, H. Iwata, “Portable and Attachable Tele-Echography Robot system: FASTele,” in Proc. Annual Int. Conf. IEEE Eng. Med. Biol. Soc., 487-490, 2010.

[7] T. Yoshida, S. Saito, S. Onogi, K. Masuda, “Position Control of Echogram Plane by Probe Scan Mechanism using Pneumatic Actuators,” in Proc. Int. Conf. Computer Assisted Radiology and Surgery, vol. 7 suppl. 1, S358, 2012.

[8] E. Boctor, A. Viswanathan, M. Choti, R. H. Taylor, “A novel closed form solution for ultrasound calibration,” in Proc. IEEE International Symposium on Biomedical Imaging, vol. 1, pp. 527-530, 2004

[9] H. Zhang, F. Banovac, A. White, K. Cleary, “Freehand 3D ultrasound calibration using an electromagnetically tracked needle,” in Proc. SPIE 6141, 61412M, 2006.

[10] E. L. Melvær, K. Morken, E. Samset, “A motion constrained crosswire phantom for tracked 2D ultrasound calibration,” Int. Journal of Computer Assisted Radiology and Surgery, vol. 7, pp. 611-620, 2011.

[11] S. Onogi, Y. Sugano, T. Yoshida, K. Masuda, “An Accurate Calibration Method of Ultrasound Images by Center Positions of a Metal Ball,” in Proc. Annual Int. Conf. IEEE Eng. Med. Biol. Soc., 468-471, 2012.